Mn–Zn soft magnetic ferrite nanoparticles synthesized from spent alkaline Zn–Mn batteries

Ping Hu [a], De'an Pan [a], Shengen Zhang [a,*], Jianjun Tian [a], Alex A. Volinsky [b]

[a] School of Materials Science and Engineering, University of Science and Technology Beijing, Beijing 100083, China
[b] Department of Mechanical Engineering, University of South Florida, Tampa, FL 33620, USA

ABSTRACT

Using spent alkaline Zn–Mn batteries as raw material, Mn–Zn soft magnetic ferrite nanoparticles are prepared by multi-step processes including acid leaching, chemical treatment of battery iron shells and citrate-nitrate precursor auto-combustion. Acid leaching and chemical treatment mechanisms are investigated. Dried gels thermal decomposition process, auto-combustion, phase composition, morphological and magnetic properties of as-prepared Mn–Zn ferrite nanoparticles are characterized by thermogravimetric and differential thermal analysis, X-ray powder diffraction, transmission electron microscopy and vibrating sample magnetometer. Synthesized Mn–Zn ferrite nanoparticles ($Mn_{0.5}Zn_{0.5}Fe_2O_4$) have pure ferrite phase, larger saturation magnetization ($M_s = 60.62$ emu g^{-1}) and lower coercivity ($H_c = 30$ Oe) compared with the same composition ferrites prepared by other techniques due to better crystallinity. Mn–Zn ferrite nanoparticles synthesis method presents a viable alternative for alkaline Zn–Mn batteries recycling.

© 2011 Elsevier B.V. All rights reserved.

1. Introduction

Alkaline zinc manganese (Zn–Mn) batteries are used in portable electronic devices such as radios, remote controls, watches, calculators, cameras, toys and in many others requiring small electric power [1–3]. The consumption of alkaline batteries continues to increase because of their versatility, low maintenance and cost, and growing demand for portable power sources [4]. After use most spent alkaline batteries (SABs) are discarded as waste. While some of them are landfilled or incinerated, instead of being collected and recycled, they pollute the environment [5].

To solve environmental problems and utilize secondary materials resources, numerous recycling technologies for SABs have been developed classified as pyrometallurgy and hydrometallurgy [6–9]. While pyrometallurgical processes have certain economic benefits, burning produces secondary pollution. Hydrometallurgical process is more comprehensive, but time and reagents consuming [10,11].

Because of iron, manganese and zinc are not only the main components of SABs. Fe, Mn and Zn are also the main elements of Mn–Zn soft magnetic ferrite. Thus SABs can be used as raw material to synthesize Mn–Zn ferrite in recent years due to its target product is not a single metal or its oxide [12,13]. Mn–Zn ferrites are extensively used in transformers, magnetic recording heads, choke coils,

noise filters, electromagnetic gadgets, information storage systems, medical diagnostic and biomedical devices because of their high magnetic permeability, saturation magnetization, dielectric resistivity and relatively low eddy current losses [14,15].

Based on previous results of soft magnetic ferrite preparation [16,17], in this paper, Mn–Zn ferrite nanoparticles ($Mn_{0.5}Zn_{0.5}Fe_2O_4$) were prepared by the auto-combustion method utilizing SABs as raw materials. Acid leaching and chemical treatment mechanisms were investigated. The combustion processes, phase structural, morphological and magnetic properties of as-prepared Mn–Zn ferrite nanopartials were also characterized.

2. Experimental procedure

Mn–Zn ferrites were obtained through a multi-step process including acid leaching, chemical treatment of iron shells and citrate-nitrate precursor auto-combustion. The experimental flow chart is given in Fig. 1. First, SABs (NANFU Battery Plant, China) used as raw materials were dismantled into scrap and powder, then the washing and magnetic separation treatment were carried out to separate the plastics and the iron shells from the dismantled substances. Residues were dried, crushed and then leached in 5 mol L^{-1} nitrate acid (HNO_3) solution containing 2.5 wt.% hydrogen peroxide (H_2O_2) with magnetic stirring at 80 °C until complete dissolution. The solution was filtered and the filtrate was analyzed for Mn and Zn concentration by atomic absorption spectroscopy (AA6800, SHI-MADZU, Japan). Iron shells became ferric nitrate Fe (NO_3)$_3$ after an extra chemical treatment. In order to prepare ferrite ($Mn_{0.5}Zn_{0.5}Fe_2O_4$), suitable amounts of analytically pure manganese nitrate, zinc nitrate and iron nitrate were added to adjust Mn, Zn and Fe concentrations. Then, an appropriate amount of citric acid was added to the solution for metal nitrates and citric acid molar balance, and its pH was adjusted to 7 with ammonia. The solution was heated to 60 °C and continuously stirred using magnetic agitation. After 4 h the solution became a homogeneous viscous gel. Then

* Corresponding author. Tel.: +86 10 6233 3375; fax: +86 10 6233 3375.
  E-mail address: zhangshengen@mater.ustb.edu.cn (S. Zhang).
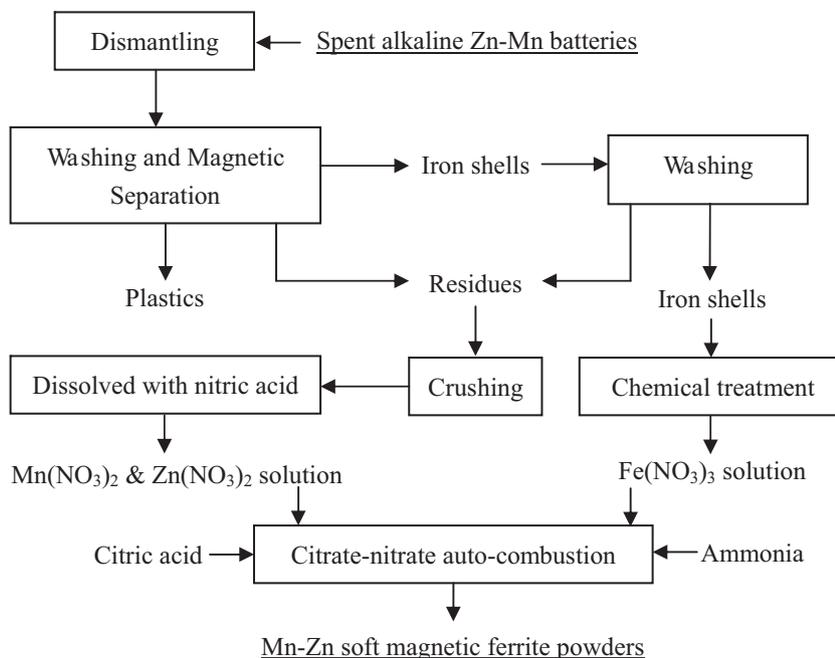
Fig. 1. Preparation flow chart of Mn–Zn soft magnetic ferrite powders obtained from SABs.

the gel was oven dried at 120 °C for 24 h to obtain a dried gel. A loose, brown and very fine Mn–Zn ferrite powder was produced after the dried gel had spontaneously combusted in air.

X-ray powder diffraction (XRD) patterns were obtained using Philips APD-10 X-ray diffractometer with Cu Kα radiation. Thermogravimetric and differential thermal analysis (METTLER TOLEDO STAR^e system, Switzerland) of the dried gel combustion product was carried out with a heating rate of 10 °C min^{-1} in air. The morphology and size of particles were observed in transmission electron microscope (Hitachi H-800, Japan). Magnetic properties measurements were carried out in a vibrating sample magnetometer (LDJ 9600, LDJ Electronics, USA).

3. Results and discussion

3.1. Chemical treatment of iron shells

In order to avoid pollution with nitrogen oxides (N_xO_y) by direct leaching iron shells with nitrate acid [14], an extra chemical treatment was carried out to convert iron shells into ferric nitrate Fe (NO_3)$_3$ environmentally friendly. At first, a leaching experiment with sulfuric acid was carried out using 3 mol L^{-1} H$_2$SO$_4$ and 2.5 wt.% H$_2$O$_2$ solutions at 60 °C. Leach liquor was filtered and the
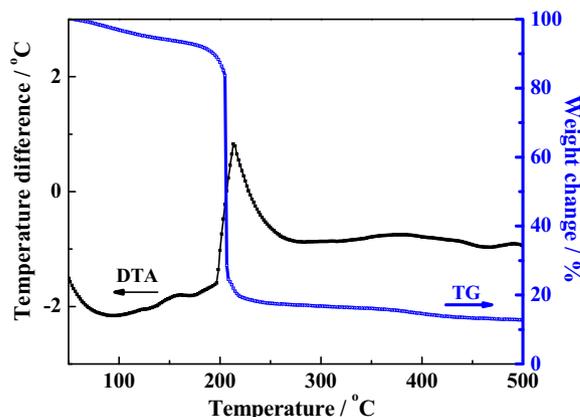
Fig. 3. TG and DTA curves of the dried gels.

filtrate was boiled for 1 h to remove residual H$_2$O$_2$. NaOH solution was added drop-by-drop for precipitation to take place during filtrate stirring to adjust the pH value in the 10–11 range. Precipitates were filtered, washed, oxidation dried and dissolved in HNO$_3$ solu-
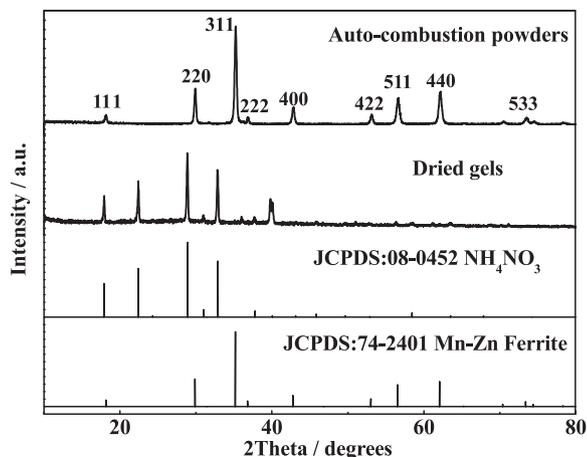
Fig. 2. XRD patterns of dried gels and auto-combustion powders.
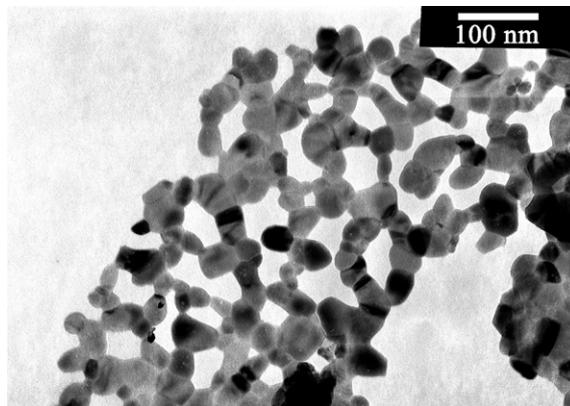
Fig. 4. TEM micrograph of prepared Mn–Zn ferrite nanoparticles.

Table 1
Mean crystallite size, magnetic properties and phases of auto-combustion Mn–Zn ferrite nanoparticles.

Sample	d_{XRD} (nm)	d_{TEM} (nm)	M_s (emu g^{-1})	M_r (emu g^{-1})	(O_e)	Phase
Mn–Zn ferrite auto-combustion nanoparticles	27 ± 2	25 ± 3	60.62	12.16	30	Mn–Zn ferrite Mn0.5Zn$_{0.5}$Fe$_2$O$_4$

tion to obtain ferric nitrate solution with the by-product sodium sulfate. Fe concentration was analyzed by atomic absorption spectroscopy. Chemical treatment reactions of iron shells are:

$$Fe + H_2SO_4 = FeSO_4 + H_2 \uparrow \tag{1}$$

$$FeSO_4 + 2NaOH = Fe(OH)_2 + Na_2SO_4 \tag{2}$$

$$4Fe(OH)_2 + O_2 + 2H_2O = 4Fe(OH)_3 \tag{3}$$

$$Fe(OH)_3 + 3HNO_3 = Fe(NO_3)_3 + 3H_2O \tag{4}$$
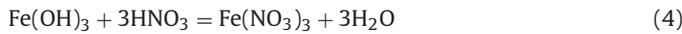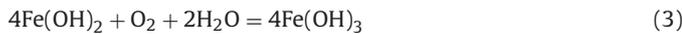
3.2. Leaching process

SABs are composed of MnO, MnO$_2$, Mn$_2$O$_3$, Mn$_3$O$_4$, ZnO within an Fe shell, as well as remnant Zn after battery discharging [18–21]. Leaching reactions of the main SABs components are:

$$4Zn + 10HNO_3 = 4Zn(NO_3)_2 + NH_4NO_3 + 3H_2O \tag{5}$$

$$ZnO + 2HNO_3 = Zn(NO_3)_2 + H_2O \tag{6}$$

$$MnO + 2HNO_3 = Zn(NO_3)_2 + H_2O \tag{7}$$

$$Mn_2O_3 + 2HNO_3 = Mn(NO_3)_2 + MnO_2 + H_2O \tag{8}$$

$$MnO_2 + 2HNO_3 + H_2O_2 = Mn(NO_3)_2 + 2H_2O + O_2 \tag{9}$$

$$Mn_3O_4 + 6HNO_3 + H_2O_2 = 3Mn(NO_3)_2 + 4H_2O + O_2 \tag{10}$$
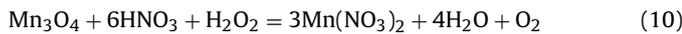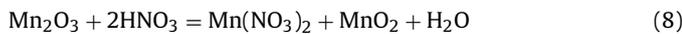
3.3. Auto-combustion for Mn–Zn ferrites synthesis

XRD patterns of dried gels and auto-combustion powders are shown in Fig. 2. The crystalline phase of the dried gels is identified to be NH$_4$NO$_3$ (JCPDS: 08-0452). As-prepared auto-combusted powder has a pure spinel Mn–Zn ferrite structure (JCPDS: 74-2401), which indicates that one can obtain pure Mn–Zn ferrite phase by the method of citrate-nitrate precursor auto-combustion from SABs. Fig. 3 shows TG and DTA curves of the dried gels. In the DTA curve, the exothermic peak is relatively sharp and intense, corresponding to abrupt weight change captured by the TG curve. Strong combustion starts at 194.76 °C, and an exothermic peak appears at 214.82 °C. Weight reduction associated with this exothermic reaction is 83.03% due to NH$_4$NO$_3$ decomposition. A great amount of heat is generated in this exothermic reaction which results
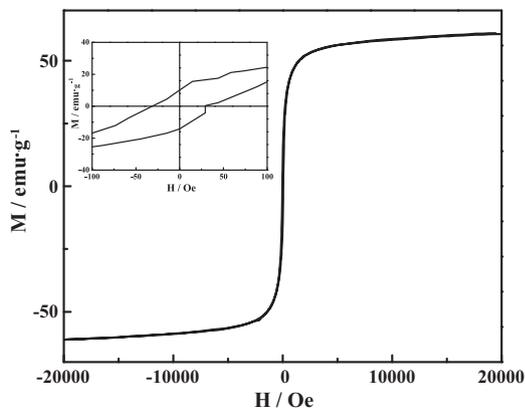
in spontaneous combustion. With further temperature increase, remaining organic compounds decompose and spinel ferrite forms. The nitrate-citrate precursor auto-combustion reaction is as follows:

$$Mn(NO_3)_2 + Zn(NO_3)_2 + Fe(NO_3)_3 + C_6H_8O_7 \cdot H_2O$$
$$+ NH_3 \cdot H_2O \rightarrow Mn_{0.5}Zn_{0.5}Fe_2O_4 \tag{11}$$
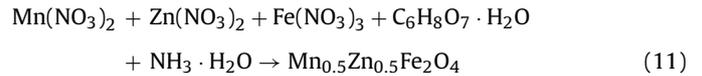
The mean crystallite size was determined using the Scherrer formula:

$$d = \frac{K\lambda}{\beta} \cdot \cos\theta \tag{12}$$

where d is the mean crystallite size, K is a constant and β is the half width of the relevant diffraction reflection, λ is the X-ray wavelength and θ is the diffraction angle. The mean crystallite size of auto-combusted powder is 27 ± 2 nm.

3.4. Mn–Zn ferrites morphology characterization

Typical TEM micrograph of prepared Mn–Zn ferrite nanoparticles' microstructure is shown in Fig. 4. Spherical Mn–Zn ferrite nanoparticles obtained from SABs are uniform in both morphology and size, but agglomerate to some extent. The average diameter of prepared Mn–Zn ferrite nanoparticles is 25 ± 3 nm, which is close to the crystallite size estimated from the Scherrer formula of the XRD pattern.

3.5. Mn–Zn ferrites magnetic properties

Magnetic properties of prepared Mn–Zn soft magnetic ferrite nanoparticles were studied using a vibrating sample magnetometer (20 kOe magnetic field) at room temperature. Magnetic hysteresis curve for Mn–Zn ferrite nanoparticles synthesized from SABs is shown in Fig. 5. Mean crystallite size, magnetic properties and phases of auto-combustion Mn–Zn ferrite nanoparticles are listed in Table 1. It is clear that synthesized Mn–Zn ferrite nanoparticles exhibit good ferromagnetic behavior. The saturation magnetization of Mn–Zn ferrite nanoparticles synthesized from SABs ($M_s = 60.62$ emu g^{-1}) is superior to the same composition ferrites prepared by other techniques [18,19]. This can be attributed to better crystallinity of the ferrite phase as seen in Fig. 2 since magnetic properties of ferrite powder strongly depend on its crystallinity and synthesis method [20,21].

4. Conclusions

Mn–Zn soft magnetic ferrite nanoparticles with the mean crystallite size of 25 nm were prepared using spent alkaline Zn–Mn batteries as raw materials by means of the multi-step processes consisting of acid leaching, chemical treatment of iron shells and citrate-nitrate precursor auto-combustion. SABs dismantling, washing, magnetic separation and crushing steps were consecutively carried out to separate batteries into iron battery shells and other dismantled substances (zinc and manganese compounds). Then these substances were dissolved in HNO$_3$ to prepare Zn (NO$_3$)$_2$ and Mn (NO$_3$)$_2$ reactant solutions. Iron shells were turned into ferric nitrate Fe (NO$_3$)$_3$ by additional chemical treatment. Mn–Zn ferrites were synthesized using citrate-nitrate precursor

Fig. 5. Magnetic hysteresis of M$_{0.5}$Zn$_{0.5}$Fe$_2$O$_4$ synthesized from SABs. The upper left inset shows a closer look of the zero-field region.

auto-combustion method. Obtained Mn–Zn ferrite nanoparticles ($Mn_{0.5}Zn_{0.5}Fe_2O_4$) have pure ferrite phase, larger saturation magnetization ($M_s = 60.62$ emu g^{-1}) and lower coercivity ($H_c = 30$ Oe) compared with the same composition ferrites prepared by other techniques due to better crystallinity. Auto-combustion Mn–Zn ferrite synthesis method is a good alternative for Zn–Mn alkaline batteries recycling.

Acknowledgments

References

[1] E. Sayilgan, T. Kukrer, G. Civelekoglu, F. Ferella, A. Akcil, F. Veglio, M. Kitis, Hydrometallurgy 97 (2009) 158–166.
[2] M.F. Almeida, S.M. Xará, J. Delgado, A.C. Costa, Waste Management 26 (2006) 466–476.
[3] M.F. Almeida, S.M. Xará, J. Delgado, A.C. Costa, Waste Management 29 (2009) 342–349.
[4] C.C.B.M. De Souza, D.C. De Oliveira, J.A.S. Tenório, Journal of Power Sources 103 (2001) 120–126.
[5] J.M. Nan, D.M. Han, M. Cui, M.J. Yang, L.M. Pan, Journal of Hazardous Materials B 133 (2006) 257–261.
[6] D.C.R. Espinosa, A.M. Bernardes, J.A.S. Tenório, Journal of Power Sources 135 (2004) 311–319.
[7] N. Vatistas, M. Bartolozzi, S. Arras, Journal of Power Sources 101 (2001) 182–187.
[8] N. Vatistas, M. Bartolozzi, Journal of Power Sources 79 (1999) 199–204.
[9] L.R.S. Veloso, L.E.O.C. Rodrigues, D.A. Ferreira, F.S. Magalhaes, M.B. Mansur, Journal of Power Sources 152 (2005) 295–302.
[10] C.H. Peng, B.S. Bai, Y.F. Chen, Waste Management 28 (2008) 326–332.
[11] A.M. Bernardes, D.C.R. Espinosa, J.A.S. Tenório, Journal of Power Sources 130 (2004) 291–298.
[12] L. Xiao, T. Zhou, J. Meng, Particuology 7 (2009) 491–495.
[13] G.X. Xi, Y.Q. Li, Y.M. Liu, Materials Letters 58 (2004) 1164–1167.
[14] G.X. Xi, L. Yang, M.X. Lu, Materials Letters 60 (2006) 3582–3585.
[15] T. Kanemaru, T. Iwasaki, S. Suda, T. Kitagawa, Preparation of ferrite from used dry cells, United States Patent 5,707,541 (1998).
[16] P. Hu, H.B. Yang, D.A. Pan, H. Wang, J.J. Tian, S.G. Zhang, X.F. Wang, A.A. Volinsky, Journal of Magnetism and Magnetic Materials 322 (2010) 173–177.
[17] H. Wang, P. Hu, D.A. Pan, J.J. Tian, S.G. Zhang, A.A. Volinsky, Journal of Alloys and Compounds 502 (2010) 338–340.
[18] M.M. Hessien, M.M. Rashad, K. El-Barawy, I.A. Ibrahim, Journal of Magnetism and Magnetic Materials 320 (2008) 1615–1621.
[19] Z.G. Zheng, X.C. Zhong, Y.H. Zhang, H.Y. Yu, D.C. Zeng, Journal of Alloys and Compounds 466 (2008) 377–382.
[20] J. Wang, K. Zhang, Z.M. Peng, Q.W. Chen, Journal of Crystal Growth 266 (2004) 500–504.
[21] A.S. Teja, P.-Y. Koh, Progress in Crystal Growth and Characterization of Materials 55 (2009) 22–45.